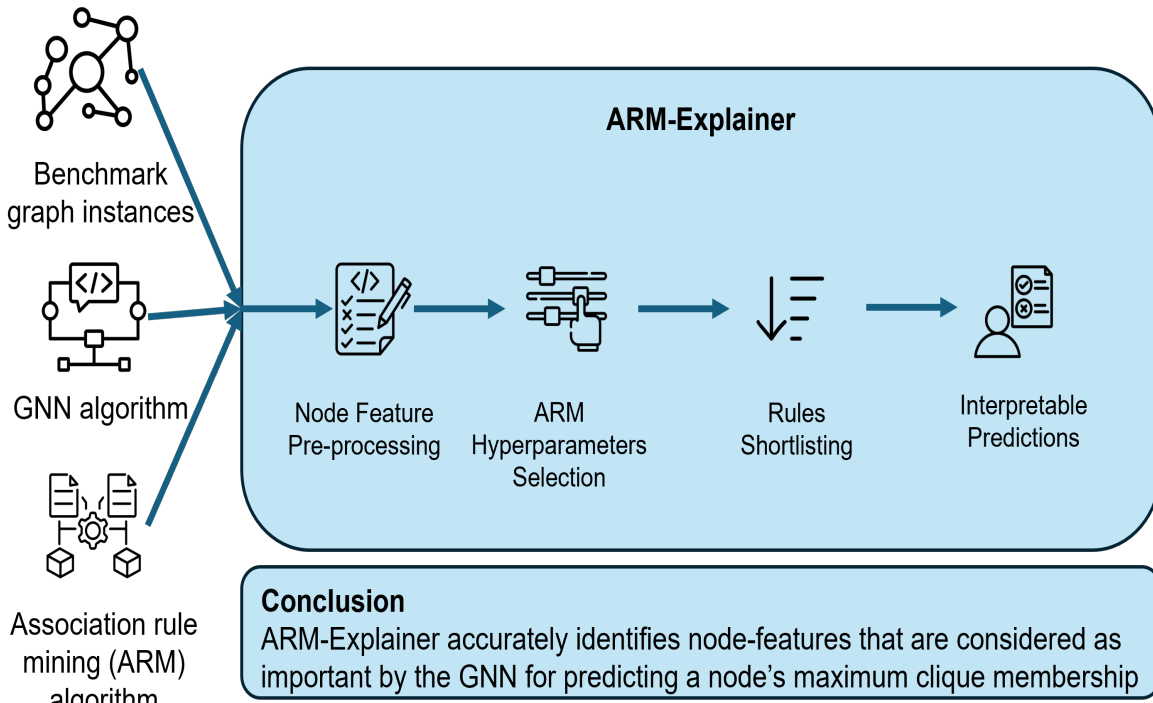


Graphical Abstract

ARM-Explainer - Explaining and improving graph neural network predictions for the maximum clique problem using node features and association rule mining

Bharat S. Sharman, Elkafi Hassini

ARM-Explainer - Explaining and improving graph neural network predictions for the maximum clique problem using node features and association rule mining



Highlights

ARM-Explainer - Explaining and improving graph neural network predictions for the maximum clique problem using node features and association rule mining

Bharat S. Sharman, Elkafi Hassini

- We introduce ARM-Explainer for explainable ML in combinatorial optimization.
- Explains predictions of a hybrid scattering GNN on the maximum clique problem.
- Adding informative node features improves GNN accuracy, especially on large graphs.
- ARM-Explainer finds key node features across inputs and graph sizes.

ARM-Explainer - Explaining and improving graph neural network predictions for the maximum clique problem using node features and association rule mining

Bharat S. Sharman^{a,1}, Elkafi Hassini^b

^a*School of Computational Science and Engineering, McMaster University, Hamilton, L8S 4E8, ON, Canada*

^b*DeGroote School of Business, McMaster University, Hamilton, L8S 4E8, ON, Canada*

Abstract

Numerous GNN-based algorithms have been proposed to solve graph-based combinatorial optimization problems (COPs). Yet, methods to explain the predictions of these algorithms for graph-based COPs have not yet been developed. This research introduces ARM-Explainer, a post-hoc, model-level explainer utilizing association rule mining, demonstrated on the hybrid geometric scattering (HGS) GNN algorithm's predictions for the maximum clique problem (MCP), a recognized NP-hard graph-based COP. The eight top explainable association rules generated by the ARM-Explainer had high median lift and confidence values of 2.42 and 0.49, respectively, on test instances from the TWITTER and BHOSLIB-DIMACS benchmark datasets. It identified the important node features and their ranges that influenced the GNN's predictions for these datasets. Moreover, incorporating informative node features into the GNN notably enhanced its predictive capability for the MCP, increasing the median largest-found clique size by 22% (from 29.5 to 36) for large graphs of the BHOSLIB-DIMACS dataset.

Keywords: Combinatorial optimization, Maximum clique problem, Graph neural networks, Association rule mining

1. Introduction

Combinatorial optimization problems (COPs) involve selecting a subset of objects from a finite set such that the selected subset optimizes an objective function defined over that set, subject to specific constraints [1]. COPs are of immense theoretical and practical importance. For example, it is well known that several COPs, such as the traveling salesperson problem (TSP), are \mathcal{NP} -hard and are widely used to formulate and solve problems in several areas, such as supply chain management [2], logistics [3], bioinformatics [4], chemical engineering [5] and cybersecurity [6], to name but a few.

A number of combinatorial optimization problems (COPs) such as the maximum clique (MCP), maximum independent set (MIS), minimum vertex cover (MVC), maximum cut (MaxCut), graph coloring (GCP), vehicle routing (VRP), and location routing (LRP) can be modeled using graphs and are collectively known as graph-based COPs. Many of these problems are \mathcal{NP} -hard, exhibiting exponential complexity in the worst-case scenario as the problem size grows. This paper focuses on the Maximum Clique Problem

¹Corresponding author: sharmanb@mcmaster.ca (Bharat S. Sharman)

(MCP), which seeks to determine the largest fully connected subgraph within a graph [7]. Karp’s seminal work [8] included the decision variant of the MCP among the initial 21 \mathcal{NP} -complete problems. The MCP is of significant theoretical and practical interest, prompting extensive research. Various methods have been proposed for solving the MCP, including exact algorithms with branch and bound (B&B) techniques [9–13], greedy and local search techniques [14–16], Monte Carlo simulations [17], and, more recently, graph neural networks (GNN) [18–20]. Approaches such as branch and bound, greedy and local search, and Monte Carlo methods are characterized by the transparency of their algorithmic steps. On the other hand, explaining the results of GNNs is challenging due to the complex transformations performed by multiple layers of neural networks on the inputs to generate the outputs. While several approaches have been proposed in the literature to explain the predictions of GNNs for a variety of node and graph classification tasks, work on the explainability of these methods for combinatorial problems has been absent [21]. To the best of the authors’ knowledge, there has been no prior work systematically explaining the predictions of the GNNs for the MCP or for graph-based COPs in general. Additionally, existing studies on GNN methods for solving graph-based COPs typically consider very few (mostly up to 3) node features in their analysis [18, 19, 22], and the effect of adding more node features on the performance of GNNs on graph-based COPs has not been investigated.

The main contributions of this study are, therefore, the following:

- Methodology for explaining the predictions of GNNs for graph-based COPs: We propose a methodology based on association rule mining (ARM) that we term ARM-Explainer to explain the predictions of GNNs for graph-based COPs. The generic nature of this methodology makes it suitable for application to a variety of GNN algorithms and graph-based COPs.
- Investigating the effect of additional node features on GNNs predictive performance for graph-based COPs : We investigate whether and to what extent the predictive performance of GNNs changes when additional node features are provided as inputs.
- Extending GNN predictions to benchmark larger graph datasets : GNN algorithms have typically been applied on smaller-sized graph benchmarks such as IMDB-BINARY and COLLAB. We extend them to larger graph benchmarks such as BHOSLIB and DIMACS.

This work seeks to offer insights into enhancing the explainability and performance of GNN predictions for graph-based COPs, targeting both academic and industrial users. The paper is structured as follows: Section 2 reviews methods for explaining GNNs. Section 3 discusses the maximum clique problem and outlines the hybrid geometric scattering (HGS) GNN algorithm used to demonstrate our method. Section 4 details the ARM-Explainer, along with datasets, node features, and computational aspects. Results are shown in section 6, while Section 7 summarizes key findings and suggests future research paths.

1.1. Graph Neural Networks (GNNs)

GNNs represent a class of neural networks adept at learning from graph-structured data. Consider an undirected, unweighted graph $G = (V, E)$, where V and E denote the set of n nodes and m edges respectively. The adjacency matrix $\mathbf{A} \in [0, 1]^{n \times n}$ for G is

defined such that $A_{ij} = 1$ if $(i, j) \in E$, otherwise 0. The nodes have features represented by the matrix $\mathbf{X} \in \mathbb{R}^{n \times F}$, where each row i of \mathbf{X} contains the F -dimensional feature vector for node i . A GNN model \mathbb{M} maps each node into a reduced-dimensional space $\mathbb{Z} = \mathbb{R}^{n \times d}$ ($d < F$) through l -step message-passing given by:

$$\mathbb{Z}_v^{l+1} = \text{UPDATE}_\Phi(\mathbb{Z}_v^l, \text{AGG}_\Psi((\text{MSG}_\Theta(\mathbb{Z}_v^l, \mathbb{Z}_u^l : (u, v) \in E))) \quad (1)$$

starting with $\mathbb{Z}^0 = \mathbf{X}$ and resulting in $\mathbb{Z} := \mathbb{Z}^l$. Various GNN architectures, including graph convolutional networks (GCN) [23], GraphSAGE [24], and graph attention networks (GAT) [25], arise from distinct combinations of update (UPDATE_Φ), aggregation (AGG_Ψ), and message generation (MSG_Θ) functions. The weights for these functions across GNN layers can be trained for diverse tasks, such as node and graph classification, link prediction, clustering, and temporal dynamics prediction.

2. Literature review

In recent years, GNN research has experienced significant expansion due to their extensive use across diverse domains, such as bioinformatics [26–28], chemical and molecular property prediction [29–43], computational fluid dynamics [44], cybersecurity [45–50], deepfake detection [51], e-commerce [52], energy [53, 54], forecasting [55], geolocation [56], medicine [57–59], natural language processing [60], neuroscience [61–65], process monitoring [66], recommender systems [67, 68], robotics [69], climate and weather prediction [70], and transportation [71]. The critical impact of predictions in domains such as healthcare, drug discovery, and cybersecurity has driven the GNN research community to create several methods to explain GNN predictions.

A comprehensive survey of GNN explainability methods has been provided in [21]. The literature survey presented here is based on this work and extends it to include new approaches that have since been proposed. Methods for explaining the predictions of GNNs can be broadly classified as factual and counterfactual. Factual algorithms aim to directly find the input features of the graph instance that have the maximum influence on the prediction of the GNN. These features can be either nodes, edges, subgraphs, higher-order structures such as cells, or a combination of these. On the other hand, counterfactual algorithms alter various features and compute the effects that these changes have on the predictions of the GNN. The features whose alteration leads to significant changes in predictions are identified as explanatory features. The explanations can be instance-level, where the explainer provides explanations for a particular graph instance, or they can be global or model-level; in which case, the explainer extracts patterns utilized by the GNN across several graphs to generate explanations. [72] Factual algorithms can be further categorized into post-hoc and self-interpretable algorithms. Post-hoc algorithms use a model that is separate from the GNN, which takes the inputs fed to the GNN, its output, and in some cases, its internal parameters, and then outputs the features that it determines are the explanatory factors behind the predictions. Different models use different parts of the inputs utilized by the GNN to determine the explanatory factors. Post-hoc algorithms can be further classified into decomposition [73–76], gradient [73, 77, 78], surrogate [72, 79–87], perturbation [82, 88–95], and generation [96–104] based methods.

Self-interpretable algorithms, on the other hand, do not have a separate module for explanation; instead, it is built into the GNN itself. When a graph instance is fed as

input to the GNN for prediction, the explanation module extracts a sub-graph from the input graph and then uses this sub-graph for both prediction and explanation. Therefore, self-interpretable algorithms have a trade-off between higher explainability and lower prediction accuracy. Self-interpretable algorithms can be further classified into those that are based on information constraints [105–110] and those that are based on structural constraints [111–115].

Counterfactual algorithms can be further classified into search-based, neural network-based, and perturbation-based algorithms, respectively. Search-based algorithms [116–120] search the counterfactual space for examples that can alter the predictions of the GNN. They are useful in situations where the prediction for an input is definitively known, and it is required to alter the input so that one obtains a different prediction. The challenge that search-based counterfactual algorithms face is that they need to be efficient, as the counterfactual search space can be exponential in size. Neural network-based algorithms [121, 122] use a neural network to generate a counterfactual instance from an existing instance. Neural networks can be used for either generating edges between nodes or generating a complete graph. Perturbation-based methods [123–130] add or delete edges to change the prediction of the GNN and do so either by altering the adjacency matrix or the computational graph of a node.

Based on the aforementioned review, this work falls into the category of factual, post-hoc methods and uses Frequent Pattern Growth (FP-Growth), an ARM method, as the surrogate model to generate model-level explanations for GNNs predictions of graph-based COPs.

3. The maximum clique problem

3.1. Definitions and notations

Let $G = (V, E)$ be an undirected and unweighted graph, where V is the set of nodes and E is the set of edges of the graph. The vertex cardinality of a graph is the number of vertices and is indicated by $|V|$, while the edge cardinality of a graph is the number of edges and is denoted by $|E|$. For a subset of nodes $S \subseteq V$, the set $G(S) = G(S, E \subseteq S \times S)$ is known as the sub-graph induced by S . A complete graph is a graph where every pair of vertices is adjacent, i.e., $\forall(i, j) \in V$; if $i \neq j$, then $(i, j) \in E$. A clique C is a complete subgraph of G . A clique is called maximal if it is not a subset of a larger clique in G . A clique is said to be the maximum clique if its vertex cardinality is the highest among all the cliques in the graph. The MCP can be formulated as the following integer linear programming problem:

$$\begin{aligned} & \text{Maximize} \quad \sum_{i \in V} x_i \\ & \text{subject to: } x_i + x_j \leq 1 \quad \forall(i, j) \notin E \\ & \quad x_i \in \{0, 1\} \quad \forall i \in V \end{aligned} \tag{2}$$

where x_i is a binary variable that indicates whether the vertex i is included in the clique ($x_i = 1$) or not ($x_i = 0$). The inequality constraint in Equation 2 specifies the condition that if there is no edge between two nodes in the graph, they cannot both be members of a clique. The clique number $\omega(G)$ is the number of vertices in the maximum clique of G . In addition to this classic version of the MCP defined on an unweighted

graph, weighted versions of the MCP also exist. If each node i of a graph has a weight w_i associated with it, these weights can collectively be represented by a weight vector $\vec{w} \in R^N$. The Maximum Weighted Clique Problem (MWCP) requires finding the clique with the maximum sum of node weights. In an analogous manner, the maximum weighted clique problem can also involve finding the clique with the maximum sum of edge weights instead of node weights. The focus of this work is on the classic version of the MCP.

3.2. Hybrid geometric scattering (HGS) algorithm

The algorithm that we considered to demonstrate our GNN explainability method is the HGS GNN proposed by [19]. HGS is a self-supervised algorithm that trains a geometric deep learning network based on a customized loss function to maximize its performance on the MCP. It was shown to achieve state of the art performance compared to EGN [18], another GNN-based algorithm, as well as mixed integer programming (MIP)-based Gurobi on graph-based COP benchmark datasets such as TWITTER [131], IMDB, and COLLAB[132]. In contrast to exact algorithms such as Gurobi [133], CliSAT [13], or MoMC [9], which use a variant of the branch-and-bound technique to directly solve Equation 2 and output the largest found clique, GNN-based algorithms such as HGS take node features as inputs and output the probability of each node being a member of a maximum clique. The transformation of node features into node probabilities is accomplished through several layers of message passing and aggregation operations. They then use a rule-based decoder to output the largest found clique by selecting a subset of fully-connected nodes, starting with the node that has the highest computed probability. Such a highly non-linear transformation between inputs and outputs leads to the black-box nature of such models, which has, in turn, motivated several approaches to explain them, as discussed in Section 2. We now provide a short introduction to the HGS algorithm. For further details, readers are referred to [19].

3.2.1. Graph scattering transform

Let $G = (V, E)$ be an undirected and unweighted graph where $V := \{v_1, v_2, \dots, v_n\}$ is the set of nodes and $E \subseteq V \times V$ is the set of edges of the graph. Let $\mathbf{W} \in R^{n \times n}$ be the adjacency matrix and $\mathbf{D} := \text{diag}\{d_1, d_2, \dots, d_n\} \in R^{n \times n}$ be the degree matrix of G , where $d_i := \sum_{j=1}^n W[v_i, v_j]$ is the degree of node i . The lazy random walk matrix can be defined as:

$$\mathbf{P} := \frac{1}{2}(\mathbf{I}_n + \mathbf{W}\mathbf{D}^{-1}) \quad (3)$$

where \mathbf{I}_n is the identity matrix. \mathbf{P} represents a diffusive process with self-retention; i.e., it models a random walker that has a nonzero probability of staying in place at a node. The graph scattering transform [134–136] is based on the lazy random walk matrix and is a wavelet-based framework for learning on graphs. In contrast to GCNs, which apply one-hop localized low-pass filters to encourage feature smoothness among adjacent nodes, the graph scattering transform employs band-pass wavelet filters that capture long-range dependencies in a graph through their large spatial support. This is accomplished by raising the lazy random walk matrix defined in Equation 3 to different powers, thereby encoding the diffusion geometry of the graph G at multiple time scales. Subsequently, subtracting such consecutive power terms from each other makes it possible to highlight variations in diffusion geometry across scales. Following the approach of [137], for $k \in \mathbb{N}_0$,

the wavelet matrix $\Psi_k \in \mathbb{R}^{n \times n}$ at scale 2^k is defined as

$$\Psi_0 = I_n - P, \quad \Psi_k = P^{2^{k-1}} - P^{2^k}, \quad k \geq 1. \quad (4)$$

Intuitively, for each node, these diffusion wavelets perform a comparison between averaged node features computed over two neighborhoods of different sizes, namely of size 2^{k-1} and 2^k . This comparison reveals how node-level information evolves as it diffuses across increasingly larger neighborhoods in the graph.

3.2.2. Components of HGS

The HGS algorithm is composed of three key elements: a GNN-based model for deriving node probabilities, an unsupervised loss function tailored to refine the probability distribution over nodes for the MCP, and a rule-based decoder designed to identify the largest clique. The following is a brief overview of these components:

1. **GNN-based training model:** The node features provided as input to the model are first embedded through an embedding module that transforms the features matrix $\mathbf{X} \in \mathbb{R}^{n \times d}$ into an embedding \mathbf{H}^0 of dimensions d_h through a multi-layer perceptron (MLP) m_{emb} , $\mathbf{H}^0 := m_{emb}(\mathbf{X})$. The authors who proposed the HGS model used three nodal features, namely eccentricity, the clustering coefficient, and the logarithm of the degree of each node as inputs. The embedding is then passed on to a diffusion module that has a series of $K \in \mathbb{N}$ diffusion layers. In each layer, the nodes have access to low-pass and band-pass filters, given by:

$$f_{low,r}(\mathbf{H}^{l-1}) = \mathbf{A}^r(\mathbf{H}^{l-1}), \quad f_{band,k}(\mathbf{H}^{l-1}) = \psi_k(\mathbf{H}^{l-1}) \quad (5)$$

In Equation 5, the low-pass filters apply the matrix $\mathbf{A} := (\mathbf{D} + \mathbf{I})^{-1/2}(\mathbf{W} + \mathbf{I})(\mathbf{D} + \mathbf{I})^{-1/2}$ raised to the power of $r \geq 1$, and the band-pass filters apply the wavelet matrix ψ_k of order k , as defined in Equation 4, to the embeddings of the layer $l-1$ respectively. The importance of each of these filters to a node is computed through an attention mechanism based computation as follows:

$$s_f^l = \sigma(\mathbf{H}_f^l || \mathbf{H}^{l-1}) \mathbf{a}^l \quad (6)$$

where $\mathbf{H}_f^l := f(\mathbf{H}^{l-1})$. The embeddings of the previous layer $l-1$ and the current layer l are computed, concatenated, and a sigmoid transformation is applied to the result. Then a learned attention vector \mathbf{a}^l is applied to the result to compute the importance score of a filter for a node. The node representations are then recomputed as:

$$\mathbf{H}_{agg}^l = \sum_{f \in F} \alpha_f^l \odot \mathbf{H}_f^l \quad (7)$$

where \odot is an element-wise multiplication operation and $\alpha_f(v) = softmax_F s_f(v)$. Such a softmax-based normalization ensures that the aggregate embedding \mathbf{H}_{agg}^l in Equation 7 comprises contributions predominantly from one filter. The aggregated embedding is then passed through an MLP (m^l) to arrive at the final node representation for that layer, i.e., $\mathbf{H}^l = m^l(\mathbf{H}_{agg}^l)$. The computed representations for all the K layers are then concatenated to obtain \mathbf{H}_{cat} , which is subsequently transformed into a vector $\mathbf{h} \in \mathbb{R}^n$ through an MLP, i.e. $\mathbf{h} = m_{out}(\mathbf{H}_{cat})$. The probability vector for nodes to belong to a maximum clique is then obtained through min-max scaling applied to \mathbf{h} , i.e., $\mathbf{p} = (\mathbf{h} - \min(\mathbf{h}) \cdot \mathbf{1}_n) / (\max(\mathbf{h}) - \min(\mathbf{h}))$.

2. **Custom supervised loss function:** To ensure that the set of nodes found is as large as possible and simultaneously satisfies the constraints of a maximum-clique, a custom loss function having two components has been proposed by the authors in [19]:

$$\mathbf{L}(\mathbf{p}) = \mathbf{L}_1(\mathbf{p}) + (\beta)\mathbf{L}_2(\mathbf{p}) = -\mathbf{p}^T \mathbf{W} \mathbf{p} + (\beta)\mathbf{p}^T \bar{\mathbf{W}} \mathbf{p} \quad (8)$$

The intuition behind such a loss function is as follows: the first component \mathbf{L}_1 assigns higher probabilities to those nodes that are highly connected. The second component has the adjacency matrix of the complement graph ($\bar{\mathbf{W}}$), which will have non-zero terms in case the nodes identified as part of a maximum clique are not connected to each other. In other words, it adds a penalty term whenever the maximum clique constraint is violated, and the relative importance of these loss terms can be adjusted by the hyperparameter β .

3. **Rule-based decoder:** Once the model has been trained using the unsupervised loss function specified in Equation 8, the output clique is finally obtained by applying a rule-based decoder. The detailed algorithmic steps of the decoder are provided [19], and a brief overview of its steps is now presented. The decoder initially orders the nodes in decreasing order of probabilities obtained after the training step. The process of building the clique starts with the first node, i.e., the one that has the highest computed probability. The decoder then goes to the second node and checks whether it is connected to the first node. If yes, it adds it to the clique set. If not, it goes to the third node, and so on. At each node, it checks whether the node is connected to all the nodes in the existing clique set. It executes this loop for a defined number of times, as determined by a hyperparameter, and when all such cliques have been found, it outputs the clique with the maximum cardinality.

4. ARM-Explainer - Explaining the predictions of HGS for the MCP using association rule mining

This section outlines ARM-Explainer, the methodology that we propose to explain the predictions of GNNs for graph-based COPs using association rule mining. Figure 1 shows the schematic of the ARM-Explainer. As a post-hoc model-level GNN explanation method, it takes in the node features of the input graphs and the predictions of a GNN for a graph-based COP, such as the MCP, and provides association rules that explain why certain nodes have been assigned high probabilities of being part of a large clique by the GNN. The graph instances and node features that we considered, a short introduction to FP-Growth, the ARM algorithm that we used, and computational considerations for the numerical experiments are now discussed.

4.1. Graph instances

The analysis was performed on two benchmark graph datasets: TWITTER [138] and BHOSLIB and DIMACS [139], which are well-known benchmarks in the GNN and combinatorial optimization research communities, respectively. A summary of these instances is provided in Table 1. A 60:20:20 split of the dataset yielded the training, validation, and test sets for the TWITTER graphs. For the BHOSLIB and DIMACS datasets, which had a comparatively fewer number of instances and greater variation in the size of graphs, the split was performed in a customized manner to ensure that graphs of different sizes were

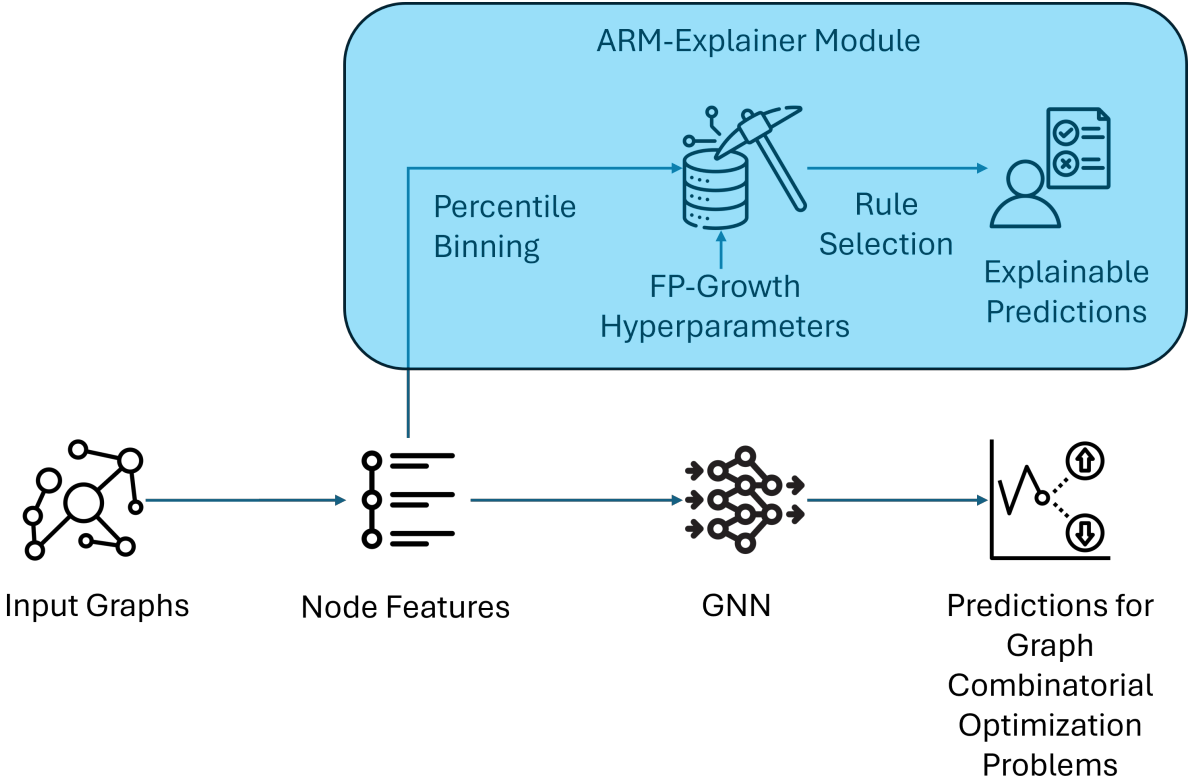


Figure 1: Illustration of the ARM-Explainer- The part highlighted in blue is the ARM-based explanation module. The node features and GNN predictions (node probabilities for belonging to a maximum clique) are used across all the graph instances are used to derive post-hoc model-level explainable rules that serve as explanations for GNN predictions

represented proportionately in the resulting training, validation, and test sets. The test set graphs of the BHOSLIB and DIMACS datasets are listed in table 3. While BHOSLIB and DIMACS constitute two separate benchmark datasets, they were considered together for this analysis, as these graphs are much larger in size and, more importantly, have a different topology compared to TWITTER graphs. For instance, all nodes across all the graphs of the BHOSLIB and DIMACS sets have a constant eccentricity (of 2), whereas it varies considerably (from 0 to 10, with a median value of 4) across nodes for TWITTER graphs. BHOSLIB and DIMACS graphs are also much denser compared to TWITTER graphs. Figures 2 and 3 show the node count, edge count, and density distributions of the training and test datasets from these two benchmarks, respectively.

Table 1: Summary of graph instances datasets used for demonstrating ARM-Explainer on the GNN predictions for the maximum clique problem

Dataset Name	Num. Training Graphs	Num. Test Graphs
TWITTER	583	196
BHOSLIB-DIMACS	76	34

4.2. Node features

The authors of HGS have considered three node features, namely eccentricity, the clustering coefficient, and the logarithm of the node degree, as inputs to the first layer of

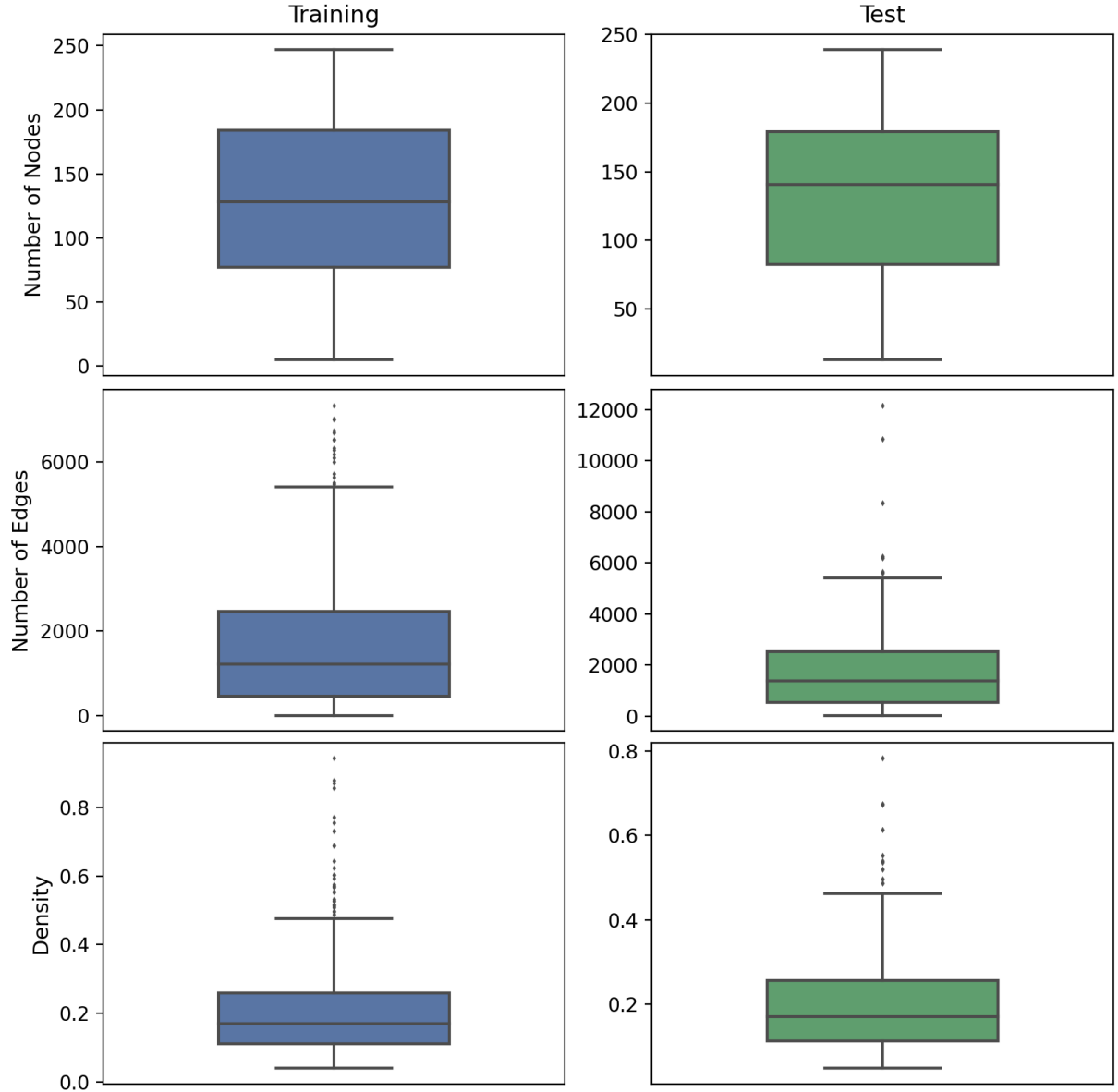


Figure 2: Node count, edge count, and density distribution of 583 training and 196 test graph instances of the TWITTER dataset

their GNN. Similarly, authors of GCON [22] have used node degree, eccentricity, clustering coefficient, and triangle counts as inputs. However, there are several other informative node features through which a GNN can potentially learn rich topological information and improve its predictions for graph-based COPs. Indeed, we observed this to be the case, particularly for the large graphs of the BHOSLIB and DIMACS datasets, where incorporating additional node features led to a significant improvement in the size of the largest clique determined by the GNN.

Ten node features were considered in this study, namely the logarithm of node degree, the logarithm of the number of triangles, clustering coefficient, eccentricity, betweenness centrality, closeness centrality, degree centrality, eigenvector centrality, the logarithm of the median of the degrees of neighboring nodes, and the logarithm of the standard deviation of the degrees of neighboring nodes. The selection of an additional four centrality-

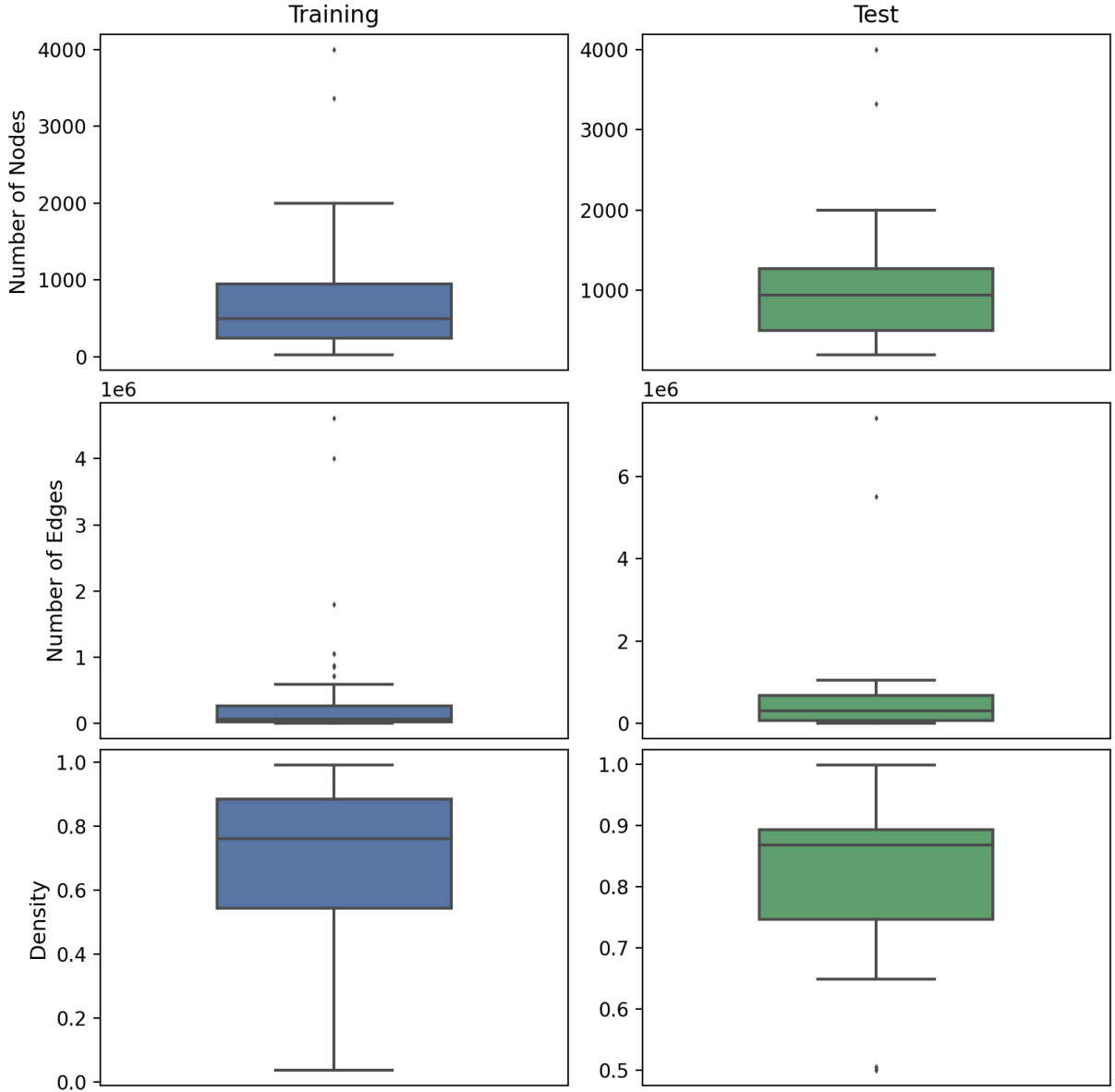


Figure 3: Node count, edge count, and density distribution of 76 training and 34 test graph instances of the BHOSLIB and DIMACS datasets

based features and two neighboring-node-based features was motivated by the reasonable assumption that nodes belonging to large cliques may have values for some of these features that are significantly different from those of the rest of the nodes in the graph—an assumption that proved to hold true, as will be shown in Section 6 when we discuss the results. The time complexities of these features are listed in Table A.5 of the Appendix. All these features are computable in polynomial time, and there are optimized recipes available to compute several of them much faster than the indicated worst case time-complexities (mentioned in the notes accompanying Table A.5. The correlations between node features for the two datasets are shown in the heatmaps of Figures A.4 and A.5, respectively, in the Appendix. It can be observed from these heatmaps that there is a significant difference between the correlation values of several node feature pairs across the two datasets, again highlighting the fact that the graphs of these two datasets have different topologies.

4.3. FP-Growth association rule mining algorithm

ARM is an important class of techniques in data mining that uncovers interesting relationships, correlations, or co-occurrences among items within large datasets. It is widely used in domains such as market basket analysis, bioinformatics, web usage mining, and social network analysis. The objective is to identify rules of the form $X \Rightarrow Y$, where X and Y are disjoint itemsets, indicating that the presence of X in a transaction implies a strong likelihood of Y also occurring. For example, in a retail dataset, the rule $\{\text{bread, butter}\} \Rightarrow \{\text{milk}\}$ suggests that customers who buy bread and butter are likely to buy milk as well. Such patterns provide actionable insights for decision-making, including cross-selling, inventory management, and recommendation systems. ARM serves as one of the important classes of methods to explain observations in both commercial and scientific contexts. Several ARM algorithms, such as Apriori [140], ECLAT [141], RELim [142], CHARM [143], and FP-Growth [144], among others, have been proposed in the literature. In this work, we have used FP-Growth to explain GNN predictions.

The FP-Growth algorithm proposed by [144] is a fast, memory-aware method for mining frequent itemsets that underpin association rules. In contrast to candidate-generation approaches such as Apriori, FP-Growth compresses the database into a compact FP-tree in two passes: (i) a scan to compute item supports and prune infrequent items; (ii) a second scan to insert transactions in a fixed frequency order so that common prefixes are merged. The rule mining process proceeds by *conditional pattern bases*: for each item, FP-Growth builds a conditional FP-tree from transactions that contain it and recursively “grows” longer patterns. This divide-and-conquer process explores only relevant regions of the search space, avoiding the combinatorial explosion typical of level-wise algorithms.

Compared to Apriori, FP-Growth eliminates the costly generate-and-test loop and repeated full scans, which is especially advantageous for dense data or low support thresholds. Relative to Eclat, which relies on vertical TID-list intersections, FP-Growth often yields better cache behavior and lower memory requirements when many items share prefixes (in dense or moderately sparse data regimes), while still remaining competitive in sparse data. Algorithms such as Relim or H-Mine share recursive ideas, but the FP-tree’s structured compression and header links typically enable faster conditional exploration with fewer intermediate structures.

As an explainable machine learning tool, FP-Growth pairs naturally with post-hoc explanation pipelines. Association rules derived from frequent itemsets provide transparent, human-readable statements parameterized by measures such as support, confidence, and lift that map complex model behavior to simple feature co-occurrences. In graph-based combinatorial optimization, such as the maximum clique problem, “items” can represent a combination of local structural indicators (e.g., percentile bins for node degrees, triangle counts, clustering coefficients, etc.) and predictions from algorithms such as GNN, including the probability of a node belonging to a maximum clique. Applying FP-Growth to these “transactions” surfaces recurrent substructures—for instance, rules of the form

$$\{\text{high triangle density}\} \Rightarrow \{\text{high probability of belonging to a large clique}\}$$

that succinctly describes the conditions under which the GNN selects nodes for large clique membership.

FP-Growth’s two-scan construction, absence of candidate generation, and focused conditional mining make it well-suited for large graph datasets, where exhaustive enumeration of subgraphs is infeasible. The resulting rule sets are compact yet expressive,

facilitating auditable insights (what structural signals the model relies on), model debugging (identifying spurious correlations), and knowledge transfer (turning opaque embeddings into domain rules). Readers interested in learning the algorithmic details of FP-Growth are referred to [144]. Thus, FP-Growth provides an effective bridge between scalable pattern mining and explainable reasoning for GNN-driven solutions to graph combinatorial optimization tasks, and it motivates the empirical analysis that follows.

4.4. *ARM-Explainer Methodology*

Figure 1 provides a schematic of the ARM-Explainer. The process of deriving explainable association rules from the node features involves the following three steps:

1. **Percentile Binning:** The node features, as well as the probability of a node belonging to a maximum clique, as predicted by the GNN, are both binned into five percentile categories: 0-20, 20-40, 40-60, 60-80, and 80-100 at the graph instance level. In other words, all the node features and the node output probabilities are transformed from their numerical values to categorical percentile values for each graph instance, with the top and bottom 20 percentile values for that graph being placed in the 80-100 and 0-20 percentile levels, respectively. While there can be other binning choices, our study found that binning by 20 percentile increments yielded results with good support and confidence measures while avoiding overfitting. It should be noted that only the nodes in the top and bottom 20 percentiles (i.e., 40 percent of the total nodes in a graph) in terms of their predicted probability values of belonging to a maximum clique from each graph instance were selected. This was done with the aim of identifying the node features that play an important role for nodes that the GNN considers to be either very likely or very unlikely to be members of a maximum clique.
2. **Setting FP-Growth Hyperparameters:** It is important to carefully select the hyperparameters of the FP-Growth algorithm to avoid generating trivial rules and a combinatorial explosion of rules. We selected a minimum support of 0.05 and a minimum confidence of 0.1 for an association rule to be selected. (Definitions of the key metrics of association rule mining are provided in Appendix B. The values of support and confidence for several rules were well above the threshold, as will be discussed in Section 6.
3. **Rule Selection:** ARM can generate hundreds of rules, and several of these rules can overlap with one another. We developed an algorithm, Greedy Selection of Non-Overlapping Association Rules (see Algorithm 1), to select non-overlapping association rules from the output. This algorithm arranges the rules in decreasing order of support and subsequently adds non-overlapping rules greedily, one-by-one, until all rules in the initial set are covered.

5. Computational experiments

The computational experiments were performed on a Linux Ubuntu 22.04.3 LTS 64 bit system, utilizing an AMD Ryzen 1920 processor with 24 threads operating at a clock speed of 4 GHZ and a TU106 GeForce RTX 2070 GPU equipped with 8 GB of memory.

Algorithm 1: Greedy Selection of Non-Overlapping Association Rules

\mathcal{R} : set of rules (columns: `antecedents`, `consequents`, and numeric metrics such as `support`, `confidence`, `lift`)

Input: c^* : target consequent value to retain
 m : name of sort metric (e.g., `support`, `confidence`, `lift`)
 $\varepsilon = 0.01$: tolerance for treating adjacent intervals as disjoint

Output: \mathcal{S} : ordered list of selected non-overlapping rules

```

1  $\mathcal{R} \leftarrow \{r \in \mathcal{R} \mid r.consequents = c^*\}$ 
2 if  $\mathcal{R} = \emptyset$  then
3   return  $\emptyset$ 
4   // Sort rules descending by the chosen metric
5  $\mathcal{S} \leftarrow []$                                 // selected rules (in order)
6  $\mathcal{F} \leftarrow []$                             // per-selected rule parsed feature-interval lists
7 foreach  $r \in \mathcal{R}$  do
8    $\mathcal{I} \leftarrow \text{ParseAntecedents}(r.antecedents)$ 
9   if  $\mathcal{I} = \emptyset$  then
10    continue
11   if  $\forall \mathcal{J} \in \mathcal{F} : \text{IsDisjoint}(\mathcal{I}, \mathcal{J}, \varepsilon)$  then
12     append  $r$  to  $\mathcal{S}$ ; append  $\mathcal{I}$  to  $\mathcal{F}$ 
13   else
14     // discard  $r$  (its feature(s) overlap with existing feature
15     // interval(s) in  $\mathcal{F}$ )
16
17 return  $\mathcal{S}$ 
18
19 Notes. PARSEANTECEDENTS turns an antecedent string into a list of
  
```

feature-interval tuples (f, ℓ, u) with percent bounds as floats. `ISDISJOINT` returns `true` iff, for every feature shared by two lists, their intervals do not overlap beyond ε ; adjacency (e.g., $[0, 19.99]$ vs. $[20, 39.99]$) is treated as disjoint.

The HGS model was trained on the TWITTER and BHOSLIB-DIMACS graphs separately, and the models providing the highest average clique sizes across all instances were selected as the models to be used for explainable machine learning using the ARM-Explainer. Four computational runs were performed—one each for the TWITTER and BHOSLIB-DIMACS datasets, and one each with 3 and 10 node features, respectively. The sets of three and ten node features were the same as described in Section 4.2. Since BHOSLIB and DIMACS graphs had the same eccentricity for all instances, this feature was not included as part of the 3 and 10 input node features; therefore, the number of node features was 2 and 9 for this dataset, respectively. The optimal hyperparameters found for the trained models, as well as the average and median number of nodes in the largest cliques identified by the trained model on the test datasets, are summarized in Table 2. It was observed that optimal results were obtained in each of the four cases when the values of the number of epochs, penalty coefficient, and learning rate were set to 12, 0.06, and 0.0004, respectively.

Table 2: Optimal hyperparameters and largest clique results for TWITTER and BHOSLIB-DIMACS test datasets

Dataset	Features	Epochs	Penalty Coefficient	Learning Rate	Average Nodes in Largest Clique	Median Nodes in Largest Clique
TWITTER	3	12	0.06	0.0004	15.11	13
TWITTER	10	12	0.06	0.0004	15.68	13
BHOSLIB-DIMACS	2	12	0.06	0.0004	68.2	29.5
BHOSLIB-DIMACS	9	12	0.06	0.0004	72.4	36

6. Results and discussion

As is evident from the columns for average and median node counts of the largest cliques found in Table 2, providing a greater number of node features as inputs does lead to improvements in GNN performance. This was especially evident for large graphs of the BHOSLIB-DIMACS dataset, where the median number of nodes in the largest clique found increased by 22% (from 29.5 to 36) across the test dataset. The instance-wise results are presented in Table 3. A positive percentage change in the size of the largest clique found was observed in 28 out of 34 test instances, and there was 1 graph instance in which a decrease was noted. Encouragingly, for graphs such as $p_{\text{hat}}500-2$, $p_{\text{hat}}1000-3$, and $p_{\text{hat}}1500-2$, which have a wider node degree spread and larger cliques than uniform graphs, the percentage change in the largest clique size found was 100% or greater. The average size of the largest clique found increased by 3.7% (from 15.11 to 15.68) for the test graphs of the TWITTER dataset.

A total of 60 association rules across both datasets were generated by the ARM-Explainer, and those with the highest lift values are presented in Table 4. The confidence values for all the rules were well above the 0.1 threshold. The support values were also well above the 0.05 threshold for 7 of the 8 rules. To illustrate the explainability of these rules, let's consider the first rule in the table. Here, for the BHOSLIB-DIMACS test instances, 3 node features are provided as inputs. There are two entries in the Consequent columns, namely $MC_{\text{Prob}}_{\text{Top}}_{20\%}$ and $MC_{\text{Prob}}_{\text{Bottom}}_{20\%}$, that represent the predicted maximum clique membership probability in the top and bottom 20 percentiles, respectively. The Antecedent columns contain node-feature-based entries along with their percentiles. So, the Log Degree in [0%, 20%] refers to the nodes that have the logarithm of their degrees within the 0 to 20 percentile range for their particular graph instances. So, as per the first rule, for BHOSLIB-DIMACS graphs, whenever the logarithm of the degrees of nodes falls in the 0 to 20 percentile bin (i.e., nodes having low degrees), there is almost a 50% confidence that the probabilities of these nodes being part of a maximum clique lie within the top 20 percentile. A lift value of 2.497 means that it is almost 2.5 times more likely that whenever the logarithm of the degrees of a node falls within the 0 to 20 percentile bin, it will have a probability of being part of a maximum clique lying within the top 20 percent as compared to the average likelihood of all nodes that have their probabilities of being part of a maximum clique lying within either the top or bottom 20 percentiles.

There are two interesting insights from the explainable rules tabulated in Table 4:

1. When we compare rules across datasets, with the number of input features being 3 (or 2 for BHOSLIB-DIMACS), we observe that, in the case of TWITTER, the nodes that have high degrees (80th to 100th percentile) are much more likely to be classified by the GNN as nodes belonging to a maximum clique. The nodes that have low degrees (0th to 20th percentile) are more likely to be classified as not belonging

Table 3: Comparison of sizes of largest cliques found by HGS using 2 and 9 node features across BHOSLIB-DIMACS test set instances.

Instances	Number of Nodes	Number of Edges	Density	Nodes in Largest Found Clique (2 features)	Nodes in Largest Found Clique (9 features)	Percentage Change in Clique Size
brock200_1	200	14834	0.7454	16	17	6%
sanr200_0.9	200	17863	0.8976	29	31	7%
C250.9	250	27984	0.8991	30	36	20%
sanr400_0.7	400	55869	0.7001	14	16	14%
dsjc500.5	500	62624	0.502	11	11	0%
p_hat500-2	500	62946	0.5046	13	26	100%
gen400_p0.9_65	400	71820	0.9	42	42	0%
gen400_p0.9_75	400	71820	0.9	39	40	3%
frb30-15-1	450	83198	0.8235	22	23	5%
frb30-15-5	450	83231	0.8239	22	26	18%
frb35-17-1	595	148859	0.8424	26	28	8%
frb35-17-2	595	148868	0.8424	26	28	8%
brock800_1	800	207505	0.6493	14	16	14%
keller5	776	225990	0.7515	18	17	-6%
frb40-19-4	760	246815	0.8557	28	32	14%
frb40-19-1	760	247106	0.8568	29	30	3%
dsjc1000.5	1000	249826	0.5002	11	12	9%
p_hat1000-3	1000	371746	0.7442	26	58	123%
frb45-21-1	945	386854	0.8673	32	36	13%
frb45-21-5	945	387461	0.8687	32	34	6%
hamming10-2	1024	518656	0.9902	500	511	2%
MANN_a45	1035	533115	0.9963	293	293	0%
p_hat1500-2	1500	568960	0.5061	20	46	130%
frb50-23-3	1150	579607	0.8773	37	38	3%
frb50-23-4	1150	580417	0.8785	36	42	17%
frb53-24-1	1272	714129	0.8834	39	40	3%
frb53-24-5	1272	714130	0.8834	39	42	8%
frb56-25-5	1400	869699	0.8881	39	44	13%
frb56-25-2	1400	869899	0.8883	41	44	7%
C2000.5	2000	999836	0.5002	12	13	8%
frb59-26-2	1534	1049648	0.8927	42	45	7%
frb59-26-5	1534	1049829	0.8929	45	45	0%
MANN_a81	3321	5506380	0.9988	654	654	0%
frb100-40	4000	7425226	0.9284	68	74	9%

to a maximum clique. This is in line with the custom loss function of Equation 8, which favors highly connected nodes as members of a maximum clique. On the other hand, for BHOSLIB-DIMACS, we observe that the situation is reversed. Here, the nodes that have low degrees (0 to 20 percentile) are more likely to be classified as belonging to a maximum clique, and vice versa. The same conclusion also holds for TWITTER graphs with 10 features and BHOSLIB-DIMACS graphs with 9 features, where antecedents are again different across these two datasets for the same node prediction. This finding shows that ARM-Explainer is able to extract dataset specific rules that highlight the features that the GNN considers important when arriving at its predictions.

- When we compare rules within the same dataset with different numbers of input features, we observe that, in the case of BHOSLIB-DIMACS, when the number of features is increased from 2 to 9, the antecedent for nodes more likely to be classified as belonging to a maximum clique changes from nodes having low degrees (0th to 20th percentile) to a high standard deviation of the degrees of the neighboring nodes (80th to 100th percentile). Such a change in the antecedent is also observed for nodes that are more likely to be classified as not belonging to a maximum clique. As is evident from the correlation heatmap in Figure A.5, the logarithm of the node degree and the logarithm of the standard deviation of the degrees of

neighboring nodes are uncorrelated, with a correlation coefficient of 0.04. Therefore, the GNN has learned new information about the nodes through this additional feature and considers it important for the graphs in this dataset. On the other hand, for graphs of the TWITTER dataset, where the improvement in predictive performance has been marginal (3.7% average increase in the number of nodes in the largest predicted clique), it is observed that while there is a change in the antecedent, the features in the antecedents corresponding to nodes more likely to be classified as belonging to a maximum clique, namely the logarithm of the node degree and the logarithm of the number of triangles, are highly correlated (correlation of 0.98), as evident in Figure A.4. A similar conclusion also holds for nodes that are more likely to be classified as not belonging to a maximum clique. Therefore, the effect of adding additional features on predictive performance depends on the graph dataset in question, and additional features seem to significantly improve performance on larger graph instances.

Table 4: Explainable association rules with highest lift values discovered by ARM-Explainer for the maximum clique problem for BHOSLIB-DIMACS and TWITTER test graph instances.

Dataset	Features	Antecedents	Consequents	Support	Confidence	Lift
BHOSLIB-DIMACS	2	Log Degree in [0%, 20%]	MC_Prob_Top_20P ^a	0.085	0.499	2.497
BHOSLIB-DIMACS	2	Log Degree in [80%, 100%]	MC_Prob_Bottom_20P ^b	0.085	0.496	2.479
BHOSLIB-DIMACS	9	Log Std Neighbor Degree in [80%, 100%]	MC_Prob_Top_20P	0.085	0.491	2.454
BHOSLIB-DIMACS	9	Log Std Neighbor Degree in [0%, 20%]	MC_Prob_Bottom_20P	0.080	0.477	2.388
TWITTER	3	Log Degree in [80%, 100%]	MC_Prob_Top_20P	0.058	0.283	1.414
TWITTER	3	Log Degree in [0%, 20%]	MC_Prob_Bottom_20P	0.094	0.481	2.403
TWITTER	10	Log Number of Triangles in [80%, 100%]	MC_Prob_Top_20P	0.067	0.327	1.636
TWITTER	10	Eigenvector Centrality in [0%, 20%]	MC_Prob_Bottom_20P	0.101	0.518	2.588

^a MC_Prob_Top_20P: Predicted maximum clique membership probability in top 20 percentile.

^b MC_Prob_Bottom_20P: Predicted maximum clique membership probability in bottom 20 percentile.

7. Conclusion and further research

This study proposes ARM-Explainer, an association rule mining-based methodology, to explain the predictions of graph neural network algorithms on graph-based combinatorial optimization problems. To the best of the authors' knowledge, this is the first study that addresses the research gap in explaining machine learning results for graph-based COPs.

To begin with, we investigated the effect of adding additional node-level features as inputs on the predictive performance of the hybrid scattering network, one of the best performing GNN algorithms on the maximum clique problem. We found that doing so improved the median largest found clique size by 22% for BHOSLIB-DIMACS, the large graphs benchmark dataset. This finding is significant, as several studies on GNN-based algorithms for COPs have mentioned that the performance of these algorithms deteriorates with the increasing size of graph instances [19], [18], [22]. Therefore, the performance of such algorithms may be significantly enhanced by providing informative node features as inputs.

We then showed how the ARM-Explainer, an ARM-based post-hoc, model-level explainer, is able to generate explainable rules for graphs of different sizes and topologies and pinpoint with high confidence the node features and their values that the GNN considers important when arriving at its predictions.

This work opens up multiple avenues for further research. First, we have demonstrated the performance of ARM-Explainer in explaining the predictions of the HGS algorithm for the MCP. However, the node features, percentile binning, hyperparameter settings, and rule selection components of our methodology are generic; therefore, ARM-Explainer can be applied to a wide variety of learning algorithms and graph-based COPs to investigate its performance in different problem-algorithm combinations. Second, while we selected FP-Growth as the ARM algorithm in this study and provided the rationale for doing so, there are newer versions of FP-Growth proposed in the literature [145], as well as other ARM approaches such as those proposed by [146, 147], that can be applied to investigate whether they yield better association rules than FP-Growth. Third, there is scope to identify the most informative node features for different graph datasets through approaches such as SHAP values. Fourth, our post-hoc level explainer still treats the GNN as a black-box, and self-interpretable approaches can be developed. However, it is not yet clear how such an architecture would look in a COP context. For example, generating a sub-graph, such as a clique, and labeling it as the explanation for the MCP solves the problem but does not explain it. Finally, the expanded set of node features that we have considered is not exhaustive, and there could be other informative features that may further improve the predictive performance. The authors anticipate investigating some of these research directions in future work and hope that the findings presented here will inspire further research on explainable machine learning for graph-based COPs.

CRediT authorship contribution statement

Bharat S. Sharman: Conceptualization, Methodology, Software, Validation, Formal analysis, Investigation, Data curation, Writing – original draft, Writing – review & editing, Visualization. **Elkafi Hassini:** Conceptualization, Methodology, Project administration, Resources, Supervision, Writing – review & editing.

Compliance with Ethical Standards:

1. **Funding:** The authors did not receive support from any organization for the submitted work.
2. **Conflict of Interest:** Bharat Sharman declares that he has no conflict of interest. Elkafi Hassini declares that has no conflict of interest.
3. **Interests:** The authors have no relevant financial or non-financial interests to disclose.
4. **Ethical Approval:** This article does not contain any studies with human participants or animals performed by any of the authors.

Data Availability The datasets analysed during the current study are available in the following repositories:

1. TWITTER: (<http://snap.stanford.edu/data>)
2. BHOSLIB and DIMACS: (<https://networkrepository.com/>)

Acknowledgments

The authors also acknowledge the authors of the HGS algorithm, who made their code openly available, which was essential for this research. This research did not receive any

specific grant from funding agencies in the public, commercial, or not-for-profit sectors.

Declaration of generative AI and AI-assisted technologies in the writing process

During the preparation of this work, the author(s) used Writefull for scientific writing to paraphrase their initial draft to improve its scientific language. After using this tool, the authors reviewed and edited the content as needed and take full responsibility for the content of the published article.

References

- [1] D. Du, P. M. Pardalos, X. Hu, W. Wu, et al., *Introduction to Combinatorial Optimization*, Springer, 2022.
- [2] E. Hassini, M. Ben-Daya, Z. Bahrour, Modeling the impact of iot technology on food supply chain operations, *Annals of Operations Research* 348 (3) (2025) 1619–1648.
- [3] B. Mansouri, R. Abdallah, S. Tamvada, E. Hassini, B. Bellino, K. Khelil, Freight gateway consolidation for purolator international using integer programming, *INFORMS Journal on Applied Analytics* 55 (3) (2025) 263–278.
- [4] E. Kaya, B. Gorkemli, B. Akay, D. Karaboga, A review on the studies employing artificial bee colony algorithm to solve combinatorial optimization problems, *Engineering Applications of Artificial Intelligence* 115 (2022) 105311.
- [5] Y. Mizuno, T. Komatsuzaki, Finding optimal pathways in chemical reaction networks using ising machines, *Physical Review Research* 6 (1) (2024) 013115.
- [6] G. Dragotto, A. Boukhtouta, A. Lodi, M. Taobane, The critical node game, *Journal of Combinatorial Optimization* 47 (5) (2024) 74.
- [7] Q. Wu, J.-K. Hao, A review on algorithms for maximum clique problems, *European Journal of Operational Research* 242 (3) (2015) 693–709.
- [8] R. M. Karp, Reducibility among combinatorial problems, in: R. E. Miller, J. W. Thatcher, J. D. Bohlinger (Eds.), *Complexity of Computer Computations: Proceedings of a Symposium on the Complexity of Computer Computations*, Springer US, Boston, MA, 1972, pp. 85–103.
- [9] C.-M. Li, H. Jiang, F. Manyà, On minimization of the number of branches in branch-and-bound algorithms for the maximum clique problem, *Computers & Operations Research* 84 (2017) 1–15.
- [10] C.-M. Li, Z. Quan, An efficient branch-and-bound algorithm based on maxsat for the maximum clique problem, in: *Proceedings of the AAAI Conference on Artificial Intelligence*, Vol. 24, 2010, pp. 128–133.
- [11] H. Jiang, C.-M. Li, F. Manyà, Combining efficient preprocessing and incremental maxsat reasoning for maxclique in large graphs, in: *Proceedings of the Twenty-Second European Conference on Artificial Intelligence*, 2016, pp. 939–947.

- [12] P. San Segundo, F. Furini, J. Artieda, A new branch-and-bound algorithm for the maximum weighted clique problem, *Computers & Operations Research* 110 (2019) 18–33.
- [13] P. San Segundo, F. Furini, D. Álvarez, P. M. Pardalos, Clisat: A new exact algorithm for hard maximum clique problems, *European Journal of Operational Research* 307 (3) (2023) 1008–1025.
- [14] Q. Wu, J.-K. Hao, F. Glover, Multi-neighborhood tabu search for the maximum weight clique problem, *Annals of Operations Research* 196 (2012) 611–634.
- [15] Y. Wang, S. Cai, M. Yin, Two efficient local search algorithms for maximum weight clique problem, in: *Proceedings of the AAAI Conference on Artificial Intelligence*, Vol. 30, 2016, pp. 805–811.
- [16] Y. Wang, S. Cai, J. Chen, M. Yin, Sccwalk: An efficient local search algorithm and its improvements for maximum weight clique problem, *Artificial Intelligence* 280 (2020) 103230.
- [17] M. C. Angelini, P. Fachin, S. de Feo, Mismatching as a tool to enhance algorithmic performances of monte carlo methods for the planted clique model, *Journal of Statistical Mechanics: Theory and Experiment* 2021 (11) (2021) 113406.
- [18] N. Karalias, A. Loukas, Erdos goes neural: an unsupervised learning framework for combinatorial optimization on graphs, *Advances in Neural Information Processing Systems* 33 (2020) 6659–6672.
- [19] Y. Min, F. Wenkel, M. Perlmutter, G. Wolf, Can hybrid geometric scattering networks help solve the maximum clique problem?, *Advances in Neural Information Processing Systems* 35 (2022) 22713–22724.
- [20] S. Sanokowski, W. Berghammer, S. Hochreiter, S. Lehner, Variational annealing on graphs for combinatorial optimization, *Advances in Neural Information Processing Systems* 36 (2024).
- [21] J. Kakkad, J. Jannu, K. Sharma, C. Aggarwal, S. Medya, A survey on explainability of graph neural networks, *arXiv preprint arXiv:2306.01958* (2023).
- [22] F. Wenkel, S. Cantürk, S. Horoi, M. Perlmutter, G. Wolf, Towards a general recipe for combinatorial optimization with multi-filter gnns, *arXiv preprint arXiv:2405.20543* (2024).
- [23] T. Kipf, Semi-supervised classification with graph convolutional networks, *arXiv preprint arXiv:1609.02907* (2016).
- [24] W. Hamilton, Z. Ying, J. Leskovec, Inductive representation learning on large graphs, *Advances in neural information processing systems* 30 (2017).
- [25] P. Veličković, G. Cucurull, A. Casanova, A. Romero, P. Lio, Y. Bengio, Graph attention networks, *arXiv preprint arXiv:1710.10903* (2017).

- [26] B. Pfeifer, A. Saranti, A. Holzinger, Gnn-subnet: disease subnetwork detection with explainable graph neural networks, *Bioinformatics* 38 (Supplement_2) (2022) ii120–ii126.
- [27] J. M. Metsch, A. Saranti, A. Angerschmid, B. Pfeifer, V. Klemt, A. Holzinger, A.-C. Hauschild, Clarus: An interactive explainable ai platform for manual counterfactuals in graph neural networks, *Journal of Biomedical Informatics* 150 (2024) 104600.
- [28] A. Mastropietro, G. De Carlo, A. Anagnostopoulos, Xgdag: explainable gene–disease associations via graph neural networks, *Bioinformatics* 39 (8) (2023) btad482.
- [29] Z. Yang, W. Zhong, L. Zhao, C. Y.-C. Chen, Mgraphdta: deep multiscale graph neural network for explainable drug–target binding affinity prediction, *Chemical science* 13 (3) (2022) 816–833.
- [30] Y. Tian, X. Wang, X. Yao, H. Liu, Y. Yang, Predicting molecular properties based on the interpretable graph neural network with multistep focus mechanism, *Briefings in bioinformatics* 24 (1) (2023) bbac534.
- [31] A. R. Aouichaoui, F. Fan, J. Abildskov, G. Sin, Application of interpretable group-embedded graph neural networks for pure compound properties, *Computers & Chemical Engineering* 176 (2023) 108291.
- [32] Y. Jian, Y. Wang, A. Barati Farimani, Predicting co2 absorption in ionic liquids with molecular descriptors and explainable graph neural networks, *ACS Sustainable Chemistry & Engineering* 10 (50) (2022) 16681–16691.
- [33] A. Kotobi, K. Singh, D. Höche, S. Bari, R. H. Meißner, A. Bande, Integrating explainability into graph neural network models for the prediction of x-ray absorption spectra, *Journal of the American Chemical Society* 145 (41) (2023) 22584–22598.
- [34] K. Low, M. L. Coote, E. I. Izgorodina, Explainable solvation free energy prediction combining graph neural networks with chemical intuition, *Journal of Chemical Information and Modeling* 62 (22) (2022) 5457–5470.
- [35] T. Xie, J. C. Grossman, Crystal graph convolutional neural networks for an accurate and interpretable prediction of material properties, *Physical review letters* 120 (14) (2018) 145301.
- [36] Z. Yang, W. Zhong, Q. Lv, C. Y.-C. Chen, Learning size-adaptive molecular substructures for explainable drug–drug interaction prediction by substructure-aware graph neural network, *Chemical science* 13 (29) (2022) 8693–8703.
- [37] R. Henderson, D.-A. Clevert, F. Montanari, Improving molecular graph neural network explainability with orthonormalization and induced sparsity, in: *International Conference on Machine Learning*, PMLR, 2021, pp. 4203–4213.
- [38] M. Proietti, A. Ragno, B. L. Rosa, R. Ragno, R. Capobianco, Explainable ai in drug discovery: self-interpretable graph neural network for molecular property prediction using concept whitening, *Machine Learning* 113 (4) (2024) 2013–2044.

- [39] Y. L. Liu, Y. Wang, O. Vu, R. Moretti, B. Bodenheimer, J. Meiler, T. Derr, Interpretable chirality-aware graph neural network for quantitative structure activity relationship modeling in drug discovery, in: Proceedings of the AAAI Conference on Artificial Intelligence, Vol. 37, 2023, pp. 14356–14364.
- [40] H. Li, S. Zhang, L. Tang, M. Bauchy, Y. Sun, Predicting and interpreting energy barriers of metallic glasses with graph neural networks, arXiv preprint arXiv:2401.08627 (2023).
- [41] J. Rao, S. Zheng, Y. Lu, Y. Yang, Quantitative evaluation of explainable graph neural networks for molecular property prediction, *Patterns* 3 (12) (2022).
- [42] A. R. Aouichaoui, F. Fan, S. S. Mansouri, J. Abildskov, G. Sin, Combining group-contribution concept and graph neural networks toward interpretable molecular property models, *Journal of Chemical Information and Modeling* 63 (3) (2023) 725–744.
- [43] M. Dai, M. F. Demirel, Y. Liang, J.-M. Hu, Graph neural networks for an accurate and interpretable prediction of the properties of polycrystalline materials, *npj Computational Materials* 7 (1) (2021) 103.
- [44] S. Barwey, V. Shankar, V. Viswanathan, R. Maulik, Multiscale graph neural network autoencoders for interpretable scientific machine learning, *Journal of Computational Physics* 495 (2023) 112537.
- [45] T. Ganz, M. Härterich, A. Warnecke, K. Rieck, Explaining graph neural networks for vulnerability discovery, in: Proceedings of the 14th ACM Workshop on Artificial Intelligence and Security, 2021, pp. 145–156.
- [46] H. He, Y. Ji, H. H. Huang, Illuminati: Towards explaining graph neural networks for cybersecurity analysis, in: 2022 IEEE 7th European Symposium on Security and Privacy (EuroS&P), IEEE, 2022, pp. 74–89.
- [47] X. Zhu, Y. Zhang, Z. Zhang, D. Guo, Q. Li, Z. Li, Interpretability evaluation of botnet detection model based on graph neural network, in: IEEE INFOCOM 2022-IEEE Conference on Computer Communications Workshops (INFOCOM WKSHPS), IEEE, 2022, pp. 1–6.
- [48] W. W. Lo, G. Kulatilleke, M. Sarhan, S. Layeghy, M. Portmann, Xg-bot: An explainable deep graph neural network for botnet detection and forensics, *Internet of Things* 22 (2023) 100747.
- [49] D. Warmsley, A. Waagen, J. Xu, Z. Liu, H. Tong, A survey of explainable graph neural networks for cyber malware analysis, in: 2022 IEEE International Conference on Big Data (Big Data), IEEE, 2022, pp. 2932–2939.
- [50] S. Cao, X. Sun, X. Wu, D. Lo, L. Bo, B. Li, W. Liu, Coca: Improving and explaining graph neural network-based vulnerability detection systems, in: Proceedings of the IEEE/ACM 46th International Conference on Software Engineering, 2024, pp. 1–13.

- [51] F. Khalid, A. Javed, H. Ilyas, A. Irtaza, et al., Dfgnn: An interpretable and generalized graph neural network for deepfakes detection, *Expert Systems with Applications* 222 (2023) 119843.
- [52] K. Amara, R. Ying, Z. Zhang, Z. Han, Y. Shan, U. Brandes, S. Schemm, C. Zhang, Graphframex: Towards systematic evaluation of explainability methods for graph neural networks, *arXiv preprint arXiv:2206.09677* (2022).
- [53] Y. Gao, S. Miyata, Y. Akashi, Interpretable deep learning models for hourly solar radiation prediction based on graph neural network and attention, *Applied Energy* 321 (2022) 119288.
- [54] A. Verdone, S. Scardapane, M. Panella, Explainable spatio-temporal graph neural networks for multi-site photovoltaic energy production, *Applied Energy* 353 (2024) 122151.
- [55] M. Li, S. Chen, Y. Shen, G. Liu, I. W. Tsang, Y. Zhang, Online multi-agent forecasting with interpretable collaborative graph neural networks, *IEEE Transactions on Neural Networks and Learning Systems* 35 (4) (2022) 4768–4782.
- [56] F. Zhou, T. Wang, T. Zhong, G. Trajcevski, Identifying user geolocation with hierarchical graph neural networks and explainable fusion, *Information Fusion* 81 (2022) 1–13.
- [57] M. Mokhtari, T. Tsang, P. Abolmaesumi, R. Liao, Echognn: explainable ejection fraction estimation with graph neural networks, in: *International Conference on Medical Image Computing and Computer-Assisted Intervention*, Springer, 2022, pp. 360–369.
- [58] Y. Gao, D. Gu, M. Zhou, D. Metaxas, Aligning human knowledge with visual concepts towards explainable medical image classification, in: *International Conference on Medical Image Computing and Computer-Assisted Intervention*, Springer, 2024, pp. 46–56.
- [59] S. Sihag, G. Mateos, C. McMillan, A. Ribeiro, Explainable brain age prediction using covariance neural networks, *Advances in Neural Information Processing Systems* 36 (2023) 46958–46988.
- [60] P. Christmann, R. Saha Roy, G. Weikum, Explainable conversational question answering over heterogeneous sources via iterative graph neural networks, in: *Proceedings of the 46th International ACM SIGIR Conference on Research and Development in Information Retrieval*, 2023, pp. 643–653.
- [61] X. Li, Y. Zhou, N. Dvornek, M. Zhang, S. Gao, J. Zhuang, D. Scheinost, L. H. Staib, P. Ventola, J. S. Duncan, Braingnn: Interpretable brain graph neural network for fmri analysis, *Medical Image Analysis* 74 (2021) 102233.
- [62] H. Cui, W. Dai, Y. Zhu, X. Li, L. He, C. Yang, Brainnnexplainer: An interpretable graph neural network framework for brain network based disease analysis, *arXiv preprint arXiv:2107.05097* (2021).

- [63] H. Cui, W. Dai, Y. Zhu, X. Li, L. He, C. Yang, Interpretable graph neural networks for connectome-based brain disorder analysis, in: International Conference on Medical Image Computing and Computer-Assisted Intervention, Springer, 2022, pp. 375–385.
- [64] K. Zheng, S. Yu, B. Chen, Ci-gnn: A granger causality-inspired graph neural network for interpretable brain network-based psychiatric diagnosis, *Neural Networks* 172 (2024) 106147.
- [65] G. Li, M. Duda, X. Zhang, D. Koutra, Y. Yan, Interpretable sparsification of brain graphs: Better practices and effective designs for graph neural networks, in: Proceedings of the 29th ACM SIGKDD Conference on Knowledge Discovery and Data Mining, 2023, pp. 1223–1234.
- [66] M. Harl, S. Weinzierl, M. Stierle, M. Matzner, Explainable predictive business process monitoring using gated graph neural networks, *Journal of Decision Systems* 29 (sup1) (2020) 312–327.
- [67] Z. Lyu, Y. Wu, J. Lai, M. Yang, C. Li, W. Zhou, Knowledge enhanced graph neural networks for explainable recommendation, *IEEE Transactions on Knowledge and Data Engineering* 35 (5) (2022) 4954–4968.
- [68] J. Shuai, L. Wu, K. Zhang, P. Sun, R. Hong, M. Wang, Topic-enhanced graph neural networks for extraction-based explainable recommendation, in: Proceedings of the 46th International ACM SIGIR Conference on Research and Development in Information Retrieval, 2023, pp. 1188–1197.
- [69] Y. Lin, A. S. Wang, E. Undersander, A. Rai, Efficient and interpretable robot manipulation with graph neural networks, *IEEE Robotics and Automation Letters* 7 (2) (2022) 2740–2747.
- [70] R. Yang, J. Hu, Z. Li, J. Mu, T. Yu, J. Xia, X. Li, A. Dasgupta, H. Xiong, Interpretable machine learning for weather and climate prediction: A review, *Atmospheric Environment* 338 (2024) 120797.
- [71] M. N. Tygesen, F. C. Pereira, F. Rodrigues, Unboxing the graph: Towards interpretable graph neural networks for transport prediction through neural relational inference, *Transportation research part C: emerging technologies* 146 (2023) 103946.
- [72] B. Armgaan, M. Dalmia, S. Medya, S. Ranu, Graphtrail: Translating gnn predictions into human-interpretable logical rules, *Advances in Neural Information Processing Systems* 37 (2024) 123443–123470.
- [73] P. E. Pope, S. Kolouri, M. Rostami, C. E. Martin, H. Hoffmann, Explainability methods for graph convolutional neural networks, in: Proceedings of the IEEE/CVF conference on computer vision and pattern recognition, 2019, pp. 10772–10781.
- [74] Q. Feng, N. Liu, F. Yang, R. Tang, M. Du, X. Hu, Degree: Decomposition based explanation for graph neural networks, *arXiv preprint arXiv:2305.12895* (2023).

- [75] T. Schnake, O. Eberle, J. Lederer, S. Nakajima, K. T. Schütt, K.-R. Müller, G. Montavon, Higher-order explanations of graph neural networks via relevant walks, *IEEE transactions on pattern analysis and machine intelligence* 44 (11) (2021) 7581–7596.
- [76] S. Lu, K. G. Mills, J. He, B. Liu, D. Niu, Goat: Explaining graph neural networks via graph output attribution, *arXiv preprint arXiv:2401.14578* (2024).
- [77] F. Baldassarre, H. Azizpour, Explainability techniques for graph convolutional networks, *arXiv preprint arXiv:1905.13686* (2019).
- [78] S. Lu, B. Liu, K. G. Mills, J. He, D. Niu, Eig-search: Generating edge-induced subgraphs for gnn explanation in linear time, *arXiv preprint arXiv:2405.01762* (2024).
- [79] S. Akkas, A. Azad, Gnnshap: Scalable and accurate gnn explanation using shapley values, in: *Proceedings of the ACM on Web Conference 2024*, 2024, pp. 827–838.
- [80] A. Duval, F. D. Malliaros, Graphsvx: Shapley value explanations for graph neural networks, in: *Machine Learning and Knowledge Discovery in Databases. Research Track: European Conference, ECML PKDD 2021, Bilbao, Spain, September 13–17, 2021, Proceedings, Part II* 21, Springer, 2021, pp. 302–318.
- [81] Q. Huang, M. Yamada, Y. Tian, D. Singh, Y. Chang, Graphlime: Local interpretable model explanations for graph neural networks, *IEEE Transactions on Knowledge and Data Engineering* 35 (7) (2022) 6968–6972.
- [82] D. Luo, W. Cheng, D. Xu, W. Yu, B. Zong, H. Chen, X. Zhang, Parameterized explainer for graph neural network, *Advances in neural information processing systems* 33 (2020) 19620–19631.
- [83] T. Pereira, E. Nascimento, L. E. Resck, D. Mesquita, A. Souza, Distill n’explain: explaining graph neural networks using simple surrogates, in: *International Conference on Artificial Intelligence and Statistics*, PMLR, 2023, pp. 6199–6214.
- [84] Y. Zhang, D. Defazio, A. Ramesh, Relex: A model-agnostic relational model explainer, in: *Proceedings of the 2021 AAAI/ACM Conference on AI, Ethics, and Society*, 2021, pp. 1042–1049.
- [85] H. Chang, J. Ye, A. Lopez-Avila, J. Du, J. Li, Path-based explanation for knowledge graph completion, in: *Proceedings of the 30th ACM SIGKDD Conference on Knowledge Discovery and Data Mining*, 2024, pp. 231–242.
- [86] S. Azzolin, A. Longa, P. Barbiero, P. Lio, A. Passerini, Global explainability of GNNs via logic combination of learned concepts, in: *The Eleventh International Conference on Learning Representations*, 2023.
URL <https://openreview.net/forum?id=OTbRTIY4YS>
- [87] Y. Zhao, Y. Xu, D. Wang, Y. Zhang, Q. Li, L. Cui, A multi-objective explanation framework for graph neural networks, *IEEE Transactions on Knowledge and Data Engineering* (2025).
- [88] N. Bui, H. T. Nguyen, V. A. Nguyen, R. Ying, Explaining graph neural networks via structure-aware interaction index, *arXiv preprint arXiv:2405.14352* (2024).

- [89] Z. Chen, J. Zhang, J. Ni, X. Li, Y. Bian, M. M. Islam, A. Mondal, H. Wei, D. Luo, Generating in-distribution proxy graphs for explaining graph neural networks, in: Forty-first International Conference on Machine Learning, 2024.
- [90] T. Funke, M. Khosla, M. Rathee, A. Anand, Zorro: Valid, sparse, and stable explanations in graph neural networks, *IEEE Transactions on Knowledge and Data Engineering* 35 (8) (2022) 8687–8698.
- [91] M. S. Schlichtkrull, N. De Cao, I. Titov, Interpreting graph neural networks for nlp with differentiable edge masking, *arXiv preprint arXiv:2010.00577* (2020).
- [92] X. Wang, Y. Wu, A. Zhang, X. He, T.-S. Chua, Towards multi-grained explainability for graph neural networks, *Advances in Neural Information Processing Systems* 34 (2021) 18446–18458.
- [93] Z. Ying, D. Bourgeois, J. You, M. Zitnik, J. Leskovec, Gnnexplainer: Generating explanations for graph neural networks, *Advances in neural information processing systems* 32 (2019).
- [94] H. Yuan, H. Yu, J. Wang, K. Li, S. Ji, On explainability of graph neural networks via subgraph explorations, in: International conference on machine learning, PMLR, 2021, pp. 12241–12252.
- [95] S. Zhang, Y. Liu, N. Shah, Y. Sun, Gstarx: Explaining graph neural networks with structure-aware cooperative games, *Advances in Neural Information Processing Systems* 35 (2022) 19810–19823.
- [96] H. Yuan, J. Tang, X. Hu, S. Ji, Xgnn: Towards model-level explanations of graph neural networks, in: Proceedings of the 26th ACM SIGKDD international conference on knowledge discovery & data mining, 2020, pp. 430–438.
- [97] X. Wang, H.-W. Shen, Gnninterpreter: A probabilistic generative model-level explanation for graph neural networks, *arXiv preprint arXiv:2209.07924* (2022).
- [98] C. Shan, Y. Shen, Y. Zhang, X. Li, D. Li, Reinforcement learning enhanced explainer for graph neural networks, *Advances in Neural Information Processing Systems* 34 (2021) 22523–22533.
- [99] W. Lin, H. Lan, B. Li, Generative causal explanations for graph neural networks, in: International Conference on Machine Learning, PMLR, 2021, pp. 6666–6679.
- [100] W. Li, Y. Li, Z. Li, J. Hao, Y. Pang, Dag matters! gflownets enhanced explainer for graph neural networks, *arXiv preprint arXiv:2303.02448* (2023).
- [101] X. Wang, H. W. Shen, Gnnboundary: Towards explaining graph neural networks through the lens of decision boundaries, in: The Twelfth International Conference on Learning Representations, 2024.
- [102] B. B. Gaines, C. Zhu, J. Bi, Explaining graph neural networks with mixed-integer programming, *Neurocomputing* (2025) 130214.

- [103] S. Saha, S. Bandyopadhyay, Graphon-explainer: Generating model-level explanations for graph neural networks using graphons, *Transactions on Machine Learning Research* (2024).
- [104] J. Hu, J. Liu, S. Dong, B. Liao, J. Liang, V. Honavar, Dgx: Uncovering general behavior of deep graph models with model-level explanation, *IEEE Transactions on Computational Biology and Bioinformatics* (2025).
- [105] R. Huang, F. Shirani, D. Luo, Factorized explainer for graph neural networks, in: *Proceedings of the AAAI conference on artificial intelligence*, Vol. 38, 2024, pp. 12626–12634.
- [106] Y. Ji, L. Shi, Z. Liu, G. Wang, Stratified gnn explanations through sufficient expansion, in: *Proceedings of the AAAI Conference on Artificial Intelligence*, Vol. 38, 2024, pp. 12839–12847.
- [107] S. Miao, M. Liu, P. Li, Interpretable and generalizable graph learning via stochastic attention mechanism, in: *International Conference on Machine Learning*, PMLR, 2022, pp. 15524–15543.
- [108] P. Müller, L. Faber, K. Martinkus, R. Wattenhofer, Graphchef: Decision-tree recipes to explain graph neural networks, in: *The Twelfth International Conference on Learning Representations*, 2024.
- [109] J. Yu, T. Xu, Y. Rong, Y. Bian, J. Huang, R. He, Graph information bottleneck for subgraph recognition, *arXiv preprint arXiv:2010.05563* (2020).
- [110] J. Yu, J. Cao, R. He, Improving subgraph recognition with variational graph information bottleneck, in: *Proceedings of the IEEE/CVF Conference on Computer Vision and Pattern Recognition*, 2022, pp. 19396–19405.
- [111] Z. Zhang, Q. Liu, H. Wang, C. Lu, C. Lee, Protgnn: Towards self-explaining graph neural networks, in: *Proceedings of the AAAI Conference on Artificial Intelligence*, Vol. 36, 2022, pp. 9127–9135.
- [112] Y.-X. Wu, X. Wang, A. Zhang, X. He, T.-S. Chua, Discovering invariant rationales for graph neural networks, *arXiv preprint arXiv:2201.12872* (2022).
- [113] A. Feng, C. You, S. Wang, L. Tassiulas, Kergnns: Interpretable graph neural networks with graph kernels, in: *Proceedings of the AAAI conference on artificial intelligence*, Vol. 36, 2022, pp. 6614–6622.
- [114] J. Deng, Y. Shen, Self-interpretable graph learning with sufficient and necessary explanations, in: *Proceedings of the AAAI Conference on Artificial Intelligence*, Vol. 38, 2024, pp. 11749–11756.
- [115] E. Dai, S. Wang, Towards self-explainable graph neural network, in: *Proceedings of the 30th ACM International Conference on Information & Knowledge Management*, 2021, pp. 302–311.
- [116] T. Chen, D. Qiu, Y. Wu, A. Khan, X. Ke, Y. Gao, View-based explanations for graph neural networks, *Proceedings of the ACM on Management of Data* 2 (1) (2024) 1–27.

- [117] C. Chhablani, S. Jain, A. Channesh, I. A. Kash, S. Medya, Game-theoretic counterfactual explanation for graph neural networks, in: Proceedings of the ACM on Web Conference 2024, 2024, pp. 503–514.
- [118] D. Numeroso, D. Bacci, Meg: Generating molecular counterfactual explanations for deep graph networks, in: 2021 International Joint Conference on Neural Networks (IJCNN), IEEE, 2021, pp. 1–8.
- [119] G. P. Wellawatte, A. Seshadri, A. D. White, Model agnostic generation of counterfactual explanations for molecules, *Chemical science* 13 (13) (2022) 3697–3705.
- [120] M. Kosan, Z. Huang, S. Medya, S. Ranu, A. Singh, Gcfexplainer: Global counterfactual explainer for graph neural networks, *ACM Transactions on Intelligent Systems and Technology* 16 (5) (2025) 1–23.
- [121] J. Ma, R. Guo, S. Mishra, A. Zhang, J. Li, Clear: Generative counterfactual explanations on graphs, *Advances in neural information processing systems* 35 (2022) 25895–25907.
- [122] M. Bajaj, L. Chu, Z. Y. Xue, J. Pei, L. Wang, P. C.-H. Lam, Y. Zhang, Robust counterfactual explanations on graph neural networks, *Advances in Neural Information Processing Systems* 34 (2021) 5644–5655.
- [123] X. Chen, R. Cai, Z. Huang, Y. Zhu, J. Horwood, Z. Hao, Z. Li, J. M. Hernández-Lobato, Feature attribution with necessity and sufficiency via dual-stage perturbation test for causal explanation, *arXiv preprint arXiv:2402.08845* (2024).
- [124] Y. Chen, Y. Bian, B. Han, J. Cheng, How interpretable are interpretable graph neural networks?, *arXiv preprint arXiv:2406.07955* (2024).
- [125] Z. Chen, F. Silvestri, J. Wang, Y. Zhang, Z. Huang, H. Ahn, G. Tolomei, Grease: Generate factual and counterfactual explanations for gnn-based recommendations, *arXiv preprint arXiv:2208.04222* (2022).
- [126] H. Kang, G. Han, H. Park, Unr-explainer: Counterfactual explanations for unsupervised node representation learning models, in: The Twelfth International Conference on Learning Representations, 2024.
- [127] A. Lucic, M. A. Ter Hoeve, G. Tolomei, M. De Rijke, F. Silvestri, Cf-gnnexplainer: Counterfactual explanations for graph neural networks, in: International Conference on Artificial Intelligence and Statistics, PMLR, 2022, pp. 4499–4511.
- [128] D. Qiu, M. Wang, A. Khan, Y. Wu, Generating robust counterfactual witnesses for graph neural networks, *arXiv preprint arXiv:2404.19519* (2024).
- [129] J. Tan, S. Geng, Z. Fu, Y. Ge, S. Xu, Y. Li, Y. Zhang, Learning and evaluating graph neural network explanations based on counterfactual and factual reasoning, in: Proceedings of the ACM web conference 2022, 2022, pp. 1018–1027.
- [130] S. Verma, B. Armgaan, S. Medya, S. Ranu, Induce: Inductive counterfactual explanations for graph neural networks, *Transactions on Machine Learning Research* (2024).

- [131] X. Yan, H. Cheng, J. Han, P. S. Yu, Mining significant graph patterns by leap search, in: Proceedings of the 2008 ACM SIGMOD international conference on Management of data, 2008, pp. 433–444.
- [132] P. Yanardag, S. Vishwanathan, Deep graph kernels, in: Proceedings of the 21th ACM SIGKDD international conference on knowledge discovery and data mining, 2015, pp. 1365–1374.
- [133] Gurobi Optimization, LLC, Gurobi Optimizer Reference Manual (2023).
URL <https://www.gurobi.com>
- [134] F. Gama, A. Ribeiro, J. Bruna, Diffusion scattering transforms on graphs, arXiv preprint arXiv:1806.08829 (2018).
- [135] D. Zou, G. Lerman, Graph convolutional neural networks via scattering, Applied and Computational Harmonic Analysis 49 (3) (2020) 1046–1074.
- [136] F. Gao, G. Wolf, M. Hirn, Geometric scattering for graph data analysis, in: International Conference on Machine Learning, PMLR, 2019, pp. 2122–2131.
- [137] R. R. Coifman, M. Maggioni, Diffusion wavelets, Applied and computational harmonic analysis 21 (1) (2006) 53–94.
- [138] J. Leskovec, A. Krevl, SNAP Datasets: Stanford large network dataset collection, <http://snap.stanford.edu/data> (Jun. 2014).
- [139] R. A. Rossi, N. K. Ahmed, The network data repository with interactive graph analytics and visualization, in: AAAI, 2015.
URL <https://networkrepository.com>
- [140] R. Srikant, R. Agrawal, Mining quantitative association rules in large relational tables, in: Proceedings of the 1996 ACM SIGMOD international conference on Management of data, 1996, pp. 1–12.
- [141] M. J. Zaki, S. Parthasarathy, M. Ogihara, W. Li, Parallel algorithms for discovery of association rules, Data mining and knowledge discovery 1 (4) (1997) 343–373.
- [142] C. Borgelt, Keeping things simple: finding frequent item sets by recursive elimination, in: Proceedings of the 1st international workshop on open source data mining: frequent pattern mining implementations, 2005, pp. 66–70.
- [143] M. J. Zaki, C.-J. Hsiao, Charm: An efficient algorithm for closed itemset mining, in: Proceedings of the 2002 SIAM international conference on data mining, SIAM, 2002, pp. 457–473.
- [144] J. Han, J. Pei, Y. Yin, Mining frequent patterns without candidate generation, ACM sigmod record 29 (2) (2000) 1–12.
- [145] Z. Wu, G. Fang, The research on the improvement of fp-growth algorithm, Artificial Intelligence Technology Research 2 (1) (2024).
- [146] K. Sabri-Laghaie, F. Momayezi, N. Ghaleshakhani, L. Maroufi, Association rule mining based approach to consider users' preferences in the energy management of smart homes, Journal of Building Engineering 104 (2025) 112361.

- [147] E. Karabulut, P. Groth, V. Degeler, Pyaerial: Scalable association rule mining from tabular data, *SoftwareX* 31 (2025) 102341.
- [148] T. Schank, D. Wagner, Finding, counting and listing all triangles in large graphs, an experimental study, in: International workshop on experimental and efficient algorithms, Springer, 2005, pp. 606–609.

Appendix A. Node features

Appendix A.1. Computational complexity of node features

Table A.5: Node-based features used for explaining GNN predictions and their computational complexity for undirected and unweighted graphs

Feature Name	Computational Complexity
Natural logarithm of node degree ²	$O(m)$
Natural logarithm of number of triangles ³	$O\left(\sum_{(u,v) \in E} \min(\deg(u), \deg(v))\right)$
Clustering coefficient ⁴	$O\left(\sum_{(u,v) \in E} \min(\deg(u), \deg(v))\right)$
Eccentricity ⁵	$O(n \cdot (n + m))$
Betweenness centrality	$O(n \cdot (n + m))$
Closeness centrality	$O(n \cdot (n + m))$
Degree centrality	$O(m)$
Eigenvector centrality (power-iteration) ⁶	$O(k \cdot (n + m))$ where k is the number of power-iteration steps until convergence.
Natural logarithm of median of neighbor degrees	$O(n + m)$
Natural logarithm of standard deviation of neighbor degrees	$O(n + m)$

Notes:

1. In the table $n = |V|$ (number of vertices) and $m = |E|$ (number of edges). For sparse graphs $m \ll n^2$ and using n, m together is customary: e.g. $O(n \cdot m)$ is written for algorithms requiring a full single-source shortest-path from each node.

²When the node degree is computed using an adjacency list.

³Based on the work of [148]

⁴The computational complexity of clustering coefficient is same as that of number of triangles.

⁵Eccentricity of node v equals the maximum shortest-path distance from v and one breadth first search per source node has the complexity of $(O(n+m))$.

⁶Eigenvector centrality is the leading eigenvector of the adjacency matrix. Using power iteration, each step costs one sparse matrix–vector multiplication (time $O(m)$), and convergence in $k = O(\log(1/\varepsilon)/(1 - |\lambda_2|/\lambda_1))$ iterations yields a total time complexity of $O(mk)$. Convergence speed depends on spectral gap and tolerance.

2. For triangle-related quantities, multiple algorithms exist: node-iterator, edge-iterator, forward algorithm, and matrix-based methods. Practical complexity is data-dependent; a common bound used for optimized algorithms is $O(m^{3/2})$ on sparse graphs.
3. When a per-node measure needs only local neighborhood aggregates (degree, neighbor-degree mean, neighbor-degree variance), the total work across the graph is roughly linear in m (sum of adjacency lengths). Sorting per-node neighbor lists increases costs and produces the extra logarithmic factor shown for medians if we use sorting rather than selection algorithms.
4. Centrality measures based on all-pairs shortest paths (closeness, eccentricity, betweenness via Brandes) are typically the most expensive; approximations exist (sampling, truncated BFS) to reduce costs in large graphs.
5. Eigenvector centrality (power iteration) costs depend on iteration count k ; preconditioning or using sparse linear algebra libraries can accelerate convergence in practice.

Appendix A.2. Correlation between node features



Figure A.4: Correlation between node features of TWITTER graphs (train and test combined).

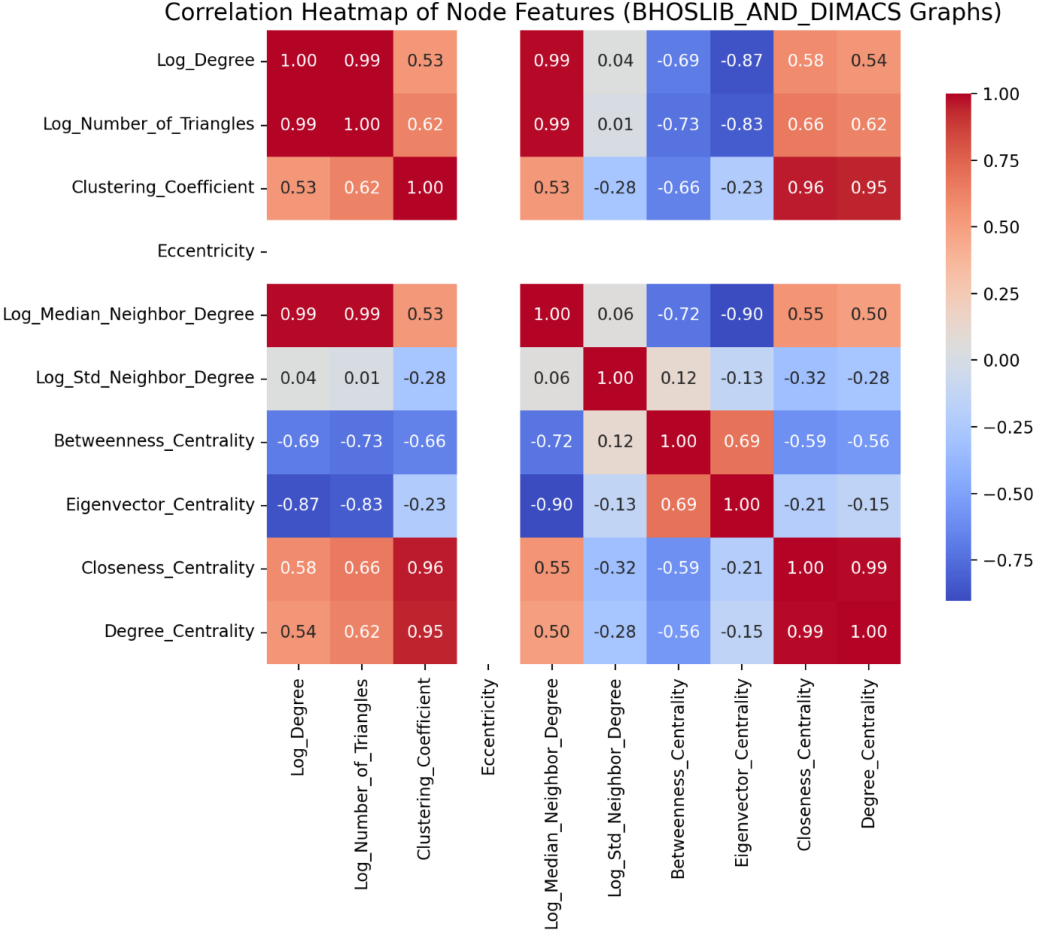


Figure A.5: Correlation between node features of BHOSLIB and DIMACS graphs (train and test combined). Since eccentricity has a constant value of 2 for all graph instances in these datasets, its correlations are omitted.

Appendix B. Association Rule Mining Terminology and Definitions

An association rule is expressed as $X \rightarrow Y$, where X (the antecedent) is a set of items and Y (the consequent) is another set, indicating that the occurrence of X suggests a likely occurrence of Y . In ARM, key metrics to assess the rule $X \rightarrow Y$ are:

- **Support:** frequency with which both X and Y occur together:

$$\text{Support}(X \rightarrow Y) = \frac{\#\{T : X \subseteq T \wedge Y \subseteq T\}}{\#\text{transactions}} = P(X \cap Y).$$

- **Confidence:** how often Y appears in transactions that contain X :

$$\text{Confidence}(X \rightarrow Y) = \frac{P(X \cap Y)}{P(X)} = P(Y | X).$$

- **Lift:** how much more likely Y is to occur with X than by random chance:

$$\text{Lift}(X \rightarrow Y) = \frac{P(Y | X)}{P(Y)} = \frac{P(X \cap Y)}{P(X) P(Y)}.$$